



Geofísica Internacional

ISSN: 0016-7169

eliedit@geofisica.unam.mx

Universidad Nacional Autónoma de
México
México

García-Ruiz, Rafael; Goguitchaichvili, Avto; López-Loera, Hector; Cervantes-Solano, Miguel; Urrutia-Fucugauchi, Jaime; Morales-Contreras, Juan; Maciel-Peña, Rafael; Rosas-Elguera, José

Paleomagnetism and Aeromagnetic Survey From Tancitaro Volcano (Central Mexico) -
Paleo-Secular Variation at Low Latitudes During the Past 1 Ma

Geofísica Internacional, vol. 56, núm. 3, julio-septiembre, 2017, pp. 287-304

Universidad Nacional Autónoma de México

Distrito Federal, México

Available in: <http://www.redalyc.org/articulo.oa?id=56851629005>

- How to cite
- Complete issue
- More information about this article
- Journal's homepage in redalyc.org

redalyc.org

Scientific Information System

Network of Scientific Journals from Latin America, the Caribbean, Spain and Portugal

Non-profit academic project, developed under the open access initiative

Paleomagnetism and Aeromagnetic Survey From Tancitaro Volcano (Central Mexico) - Paleo-Secular Variation at Low Latitudes During the Past 1 Ma

Rafael García-Ruiz, Avto Goguitchaichvili*, Hector-López Loera, Miguel Cervantes-Solano, Jaime Urrutia-Fucugauchi, Juan Morales-Contreras, Rafael Maciel-Peña and José Rosas-Elguera

Received: October 17, 2016; accepted: April 28, 2017; published on line: July 01, 2017

Resumen

El volcán Tancitaro (TV) forma parte del campo volcánico monogenético Michoacán-Guanajuato (MGVF) en el sector centro-oeste del Eje Volcánico Trans Mexicano (TMVB). Los resultados de un estudio paleo magnético de flujos de lava del volcán Tancitaro fechados radiométricamente, se utilizaron para investigar la variación paleo secular (PSV) y el campo promedio temporal (TAF) para latitudes bajas. El rango de fechado Ar-Ar fue de 70 a 960 kaños considerando los Chrones de polarización de Brunhes y Matuyama. Todas las muestras arrojaron una polaridad de magnetización normal bien definida. Dos flujos se correlacionaron con la polaridad del Evento Jaramillo, lo cual provee un marcador útil para la actividad volcánica en el MGVF. Para los análisis del PSV y TAF las paleo direcciones se combinaron con resultados anteriores de alta precisión. El estudio aeromagnético alrededor del volcán Tancitaro se caracterizó por una serie de anomalías tanto positivas como negativas. El Volcán Tancitaro presenta una gran anomalía positiva que sugiere la presencia de una gran fuente subterránea. El análisis espectral de este campo anómalo da una estimación promedio hacia la parte alta de los cuerpos que la originan entre 2-3 km.

Palabras clave: Variación paleo secular; Dipolo axial geomagnético; excursiones al Jaramillo; Volcán Tancitaro; Aeromagnetismo.

Abstract

The Tancitaro volcano (TV) is part of the Michoacan-Guanajuato monogenetic volcanic field (MGVF) in the central-western sector of the Trans-Mexican Volcanic Belt (TMVB). Results of a paleomagnetic study of radiometrically dated lava flows from Tancitaro volcano were used to investigate the paleosecular variation (PSV) and time averaged field (TAF) at low latitudes. Ar-Ar dates range from ~70 to 960 kyr spanning the Brunhes and Matuyama polarity chrons. All samples yielded well defined normal polarity magnetization. Two flows are correlated to the Jaramillo polarity event, which provide a useful marker for the volcanic activity in the MGVF. For the PSV and TAF analysis, paleodirections were combined with previously reported high standard results. The aeromagnetic survey around the Tancitaro volcano was characterized by a trend of regional anomalies over the volcanic structures. The residual field showed several positive and negative anomalies. The Tancitaro volcano is marked by a broad positive anomaly suggesting the presence of a large underground source. Spectral analysis of this anomaly field gives an average estimate to the top of the source bodies between 2-3km.

Key words: Paleosecular variation, Geomagnetic Axial Dipole, Jaramillo excursions, Tancitaro volcano, Aeromagnetism.

R. García-Ruiz
A. Goguitchaichvili*
J. Urrutia-Fucugauchi
J. Morales-Contreras
Instituto de Geofísica-Unidad Michoacán
Universidad Nacional Autónoma de México
Campus Morelia, Morelia Michoacán
Antigua Carretera a Pátzcuaro 8701, 58059, México
*Corresponding author: avto@geofisica.unam.mx

H. López-Loera
División de Geociencias Aplicadas
IPICYT, San Luis Potosí, México.

M. Cervantes-Solano
Escuela Nacional de Estudios Superiores
Unidad Morelia, Antigua Carretera a Pátzcuaro 8701
Morelia Michoacán 58190, México.

R. Maciel-Peña
Instituto Tecnológico Superior de Tacámbaro División
de Investigación y Estudios Superiores
Av. Tecnológico 201
Tacámbaro Michoacán 61650 México

J. Rosas-Elguera
Laboratorio Interinstitucional de Magnetismo Natural
Sede Guadalajara
Universidad de Guadalajara, México

Introduction

Study of radiometrically dated lava flows permits understanding the behavior of the Earth magnetic field (EMF) during the geological periods. The paleomagnetic records provide valuable information about the directions and intensity stored in each independent cooling unit. Sediments may provide quite continuous records of magnetic field variation, while lavas, due to the sporadic character of volcanic eruptions, yield rather discontinuous records of geomagnetic field fluctuations. On the other hand, the results obtained from lavas are generally more reliable because of nature and physical principles of the thermoremanent magnetization (TRM) acquisition (Prévot *et al.*, 1985). Many high resolution volcanic records have documented polarity transitions and intervals of constant polarity termed chrons and relatively short duration of 10^3 – 10^4 year's events or excursions inside. The transitional episodes are generally defined in terms of a deviations in intervals less than 10^3 years of the Virtual Geomagnetic Pole (VGP) position from the Geomagnetic Axial Dipole (GAD).

The whole Trans Mexican Volcanic Belt (TMVB) represents an excellent target for high standard paleomagnetic studies since it offers more than 3000 Plio-Quaternary lava flows (mainly monogenetic volcanoes) being many of them radiometrically dated using either K-Ar or Ar-Ar systematics. The present investigation is aimed to contribute to the Time Averaged Field (TAF) study for the past *My* and improve knowledge on the paleosecular variation (PSV) at low latitudes (20°) extending the previous work of Maciel *et al.* (2009) from Tancitaro volcano and the surrounding Michoacán-Guanajuato Volcanic Field (VFMG).

Johnson *et al.* (2008) analysis of a new generation of paleomagnetic data provides new insights about the latitudinal dependence of VGP (Virtual Geomagnetic Pole) scatter showing that this relationship is much less comparing to previous studies (Tauxe and Kent, 2004). It appears that the latitude dependence of VGP angular dispersion depends critically on a dataset from the moderate latitudes about 20° north including numerous data from Hawaii and Central Mexico. In other hand, modeling of the aeromagnetic anomalies in the area permits to investigate the subsurface structure, and stratigraphy, in particular about distribution of magnetic sources related to magmatic bodies and volcanic structures.

Geological setting and sampling details

Tancitaro volcano (TV) is an andesitic-dacitic stratovolcano located in the Michoacán-Guanajuato volcanic Field (MGVF). The MGVF has an extension of 40,000 km² and is part of the central portion of the TMVB. The MGVF has geographic boundaries $18^\circ45'N$ and $20^\circ15'N$ in latitude and $100^\circ25'W$ and $102^\circ45'W$ longitude; contains over 2000 small-sized monogenetic volcanoes including basaltic monogenetic cinder cones (Hasenaka and Carmichael, 1985), maars, tuff rings, lava domes and lava flows with hidden vents. Volcanic products are predominant calc-alkaline, but some alkaline and transitional rocks are present. Silica content varies from 47% to 70% for olivine basalt and basalt-andesite rocks (Hasenaka, 1994; Hasenaka *et al.*, 1994).

The TV is a highest stratovolcano in the MGVF with a height of 3840 mts (Ownby *et al.*, 2007), and has a large amount of dated flows. The activity start $\geq 793 \pm 22$ kyr, and its last eruption was around 237 ± 4 kyr, most of these events were dated by the radiometric method Ar^{40}/Ar^{39} (Ownby *et al.*, 2007; 2010). The present study sampled 8 lava flows to complement previous work made by Maciel *et al.* (2009). These lava flows (Figure 1) have been reported by Ownby *et al.* (2010) who present 39 new Ar-Ar dates that complement 26 flows with radiometric age also reported by Ownby *et al.*, (2007).

For the present study, the volcanic flows correspond to those with radiometric age, easy access, and sampled roadside of almost continuous structures of lava flows not being rotated or unaltered outcrops and not being near a geological fault which was corroborated with the geological map of the National Geological Service. The eight samples were obtained with a gasoline powered portable drill, oriented with a magnetic compass to obtain several samples along each flow $N \geq 8$.

The eight flows sampled cover an age range of ~ 70 to 957 kyr, and complements previous work by Maciel *et al.*, 2009, that included 11 flows with an age range from 82 to 612 kyr, since the TV is an important source of unrecorded flows that could provide important paleomagnetic information with aged of a good accuracy.

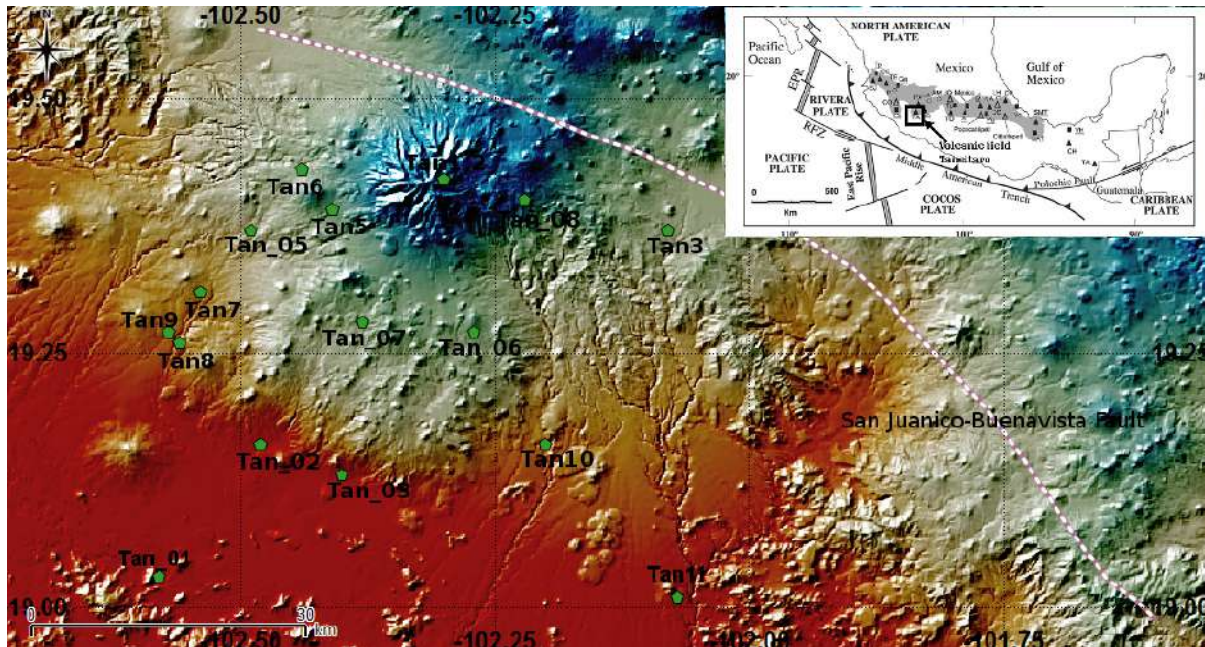


Figure 1. Location of the Tancitaro Volcano in the western sector of the TMVB showing the setting of sites reported in this study (Tan_01-08) and the previously sampled flows by Maciel *et al.*, (2014) (Tan1-11).

Magnetic Measurements and Data Analysis

Remanence measurements

All specimens were demagnetized by peak alternating fields which proved to be highly efficient to isolate the characteristic, primary remanence. A Molspin AF-demagnetizer with available alternating fields from 5 to 95 *mT* was used while magnetization was measured with a JR6A (AGICO) spinner magnetometer with nominal sensitivity $\sim 10^{-9} \text{ Am}^2$. The determination of the main magnetization components for each specimen was achieved with the method of principal component analysis (Kirschvink, 1980) and the directions were averaged by unit based on Fisher statistics (Fisher, 1953).

In most of the cases a stable, uni-vectorial characteristic remanent magnetization (ChRM) was observed (Figure 2 a) for Tan1 and Figure 2 d) for Tan7) occasionally accompanied by a negligible viscous overprint (Figure 2 b) for Tan 2 and Tan5) easily removed after the first step of demagnetization (Figure 2). Most of the specimens were completely demagnetized until 100 *mT*. The site mean directions are quite precisely determined since all α_{95} are found less than 10° . For one out to eight studied lava flows (Tan4) not paleodirection are determined due the erratic and unstable behavior during the magnetic cleaning of specimens.

The other seven volcanic flows gave stable paleodirections, and were divided in two groups, the first group are all the directions that belong to the chron of Brunhes (5 of the 7 paleodirections) and the second group are the paleodirections that belong to the chrons of Matuyama. The directions that belong to the chron of Matuyama had the peculiarity to correspond to the same event of transition due the normal polarity and the radiometric age assigned to these flows by Ownby *et al.* (2010). The transitional event known as Jaramillo, was first recognized by Doell and Dalrymple (1966).

Rock magnetism

The acquisition of thermomagnetic curves for representative samples are reported on Figure 3. Curie temperatures were estimated using the differential method of Tauxe (1998) for the analysis of the Magnetic vs Temperature curves. These analyses evidenced the low temperature phase in the heating process (red line Figure 3) T_c 492°C for sample 94T002A corresponding to site Tan_01 (Figure 3a) with two phases in the heating process (red line) that may indicates the presence of Titanomagnetite with medium Ti content. Using the method of Moskowitz (1981), it results that the highest Curie temperatures are 591°C for 94T016A corresponding to site Tan_02 (Figure 3b), and 511°C for 94T028A corresponding to Tan_03 (Figure 3c). In some cases the heating and

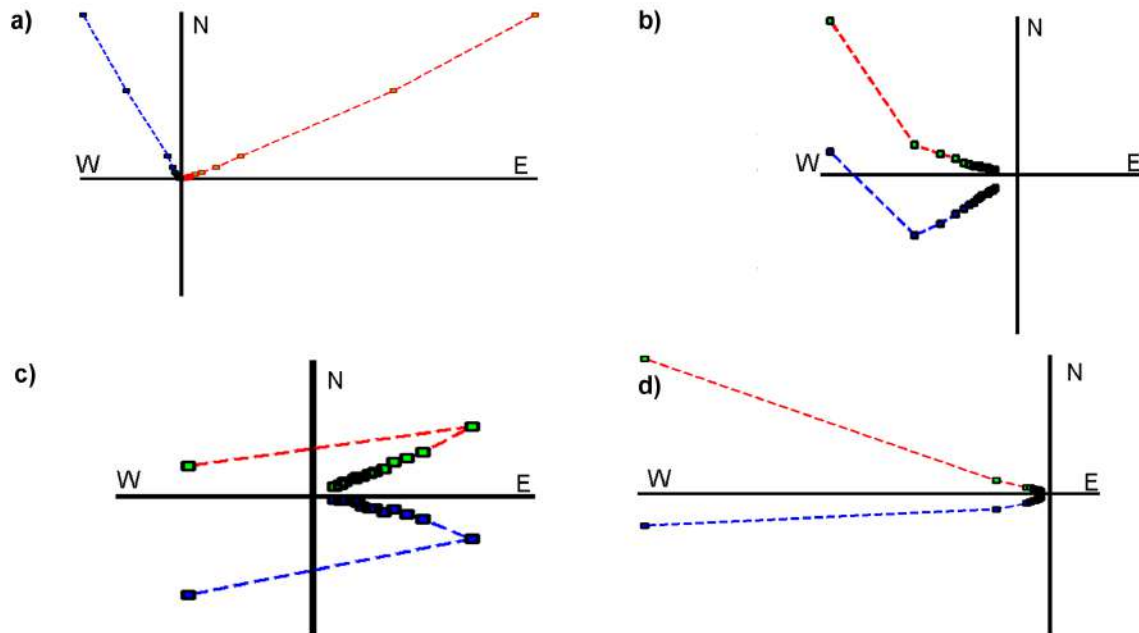


Figure 2. Representative examples of demagnetization experiments using peak alternative fields up to 95 mT, with the orthogonal vector plots, (Zijderveld diagrams) a) For the sample 94T004A and the site Tan1 b) Sample 94T015A and site Tan_02, c) Sample 94T047A corresponding to Tan_05 and d) Sample 94T060A for the site Tan_07.

cooling curves are not perfectly reversible (Tan_01). This may be due to the high to moderate mineralogical alteration at high temperatures occurred during the laboratory heating.

The hysteresis loops were analyzed using a RockMagAnalyzer1.0 software (Leonhard, 2006). Near to the origin, there is no evidence of wasp-waisted behavior (Tauxe, 1998), which reflect restricted coercivity ranges. When judging the ratios obtained from the hysteresis curves, samples fall in the pseudo-single domain PSD field (Figure 3). Isothermal remanence acquisition curves are sensitive to the magnetic mineralogy, concentration and grain size properties. Almost all samples are saturated at about 300 mT applied magnetic field, which indicate the presence of ferromagnetic phase with moderate coercivity as may be expected from magnetite and titanomagnetite grains (Tauxe, 1998). The lack of total symmetry on the hysteresis plots is generally attributed to the instrumental errors except for the study performed by Chandra *et al.* (2012) where the exchange bias seem to be the principal cause.

Main Results and Discussion

All lava flows associated to the TV yielded a normal polarity magnetization. The paleodirections were divided in two groups, five of them (Tan_01, Tan_02, and Tan_06-08) correspond to Brunhes Chron, and the other two (Tan_03 and Tan_05) belong to Matuyama Chron.

The mean paleodirection obtained from the seven flows is , , with an uncertainty $\alpha_{95}=8.21^\circ$ and $\kappa=13.89$, which correspond to the pole position of $Plat=83.06^\circ$, $Plong=294.86^\circ$, $A95=14.49^\circ$. These paleodirections are combined with those obtained by Maciel *et al.* (2009) that reported 11 normal polarity directions within normal Brunhes Chron (Table 1, Figures 4 and 5). For the global mean calculation purpose we selected sites with $N > 4$ samples per site and $\alpha_{95} \leq 10^\circ$. Moreover, transitional polarity data are rejected as common in studies of paleosecular variation (PSV) and time average field (TAF) for an age less than 5 Myr (Johnson *et al.*, 2008, Ruiz-Martínez *et al.*, 2010) to obtain a mean calculation.

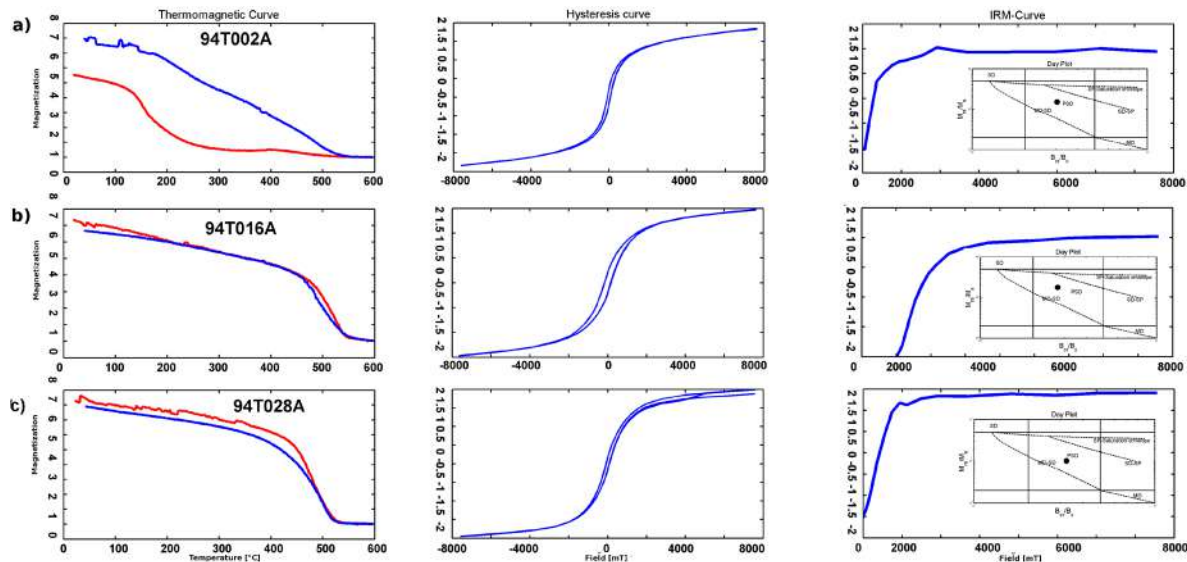


Figure 3. A summary of rock-magnetic experiments for the most representative samples: Temperature dependence of magnetization (magnetization), the red curve represent the heating process and the blue the cooling curve. Hysteresis loops for an induced magnetic field in blue (magnetization). Isothermal remanence magnetization acquisition curves (IRM), obtained with Variable Field Translation Balance with the respective Day Plot (Dunlop, 2002), to estimate the domain state of magnetic carriers and the relation of the ratios of the hysteresis parameters for the remained samples.

Table 1. Summary of all the data used in this article. Site: are the label of the sampled site; Dec and Inc: are the paleodirection treated in this study; k and a95: parameters of quality within the cone of 95%; N: Is the number of samples used to obtain the paleodirection; latitude and longitude are the coordinates for each one of the sampled sites. Age: represent the age obtained by the Ar-Ar method with its respective dispersion; VGP: are the virtual geomagnetic pole for latitude and longitude; Ref: Differentiate the paleo-direction of this study (T.S) and the paleodirection obtained by Maciel *et al.* (2014).

Site	Dec(°)	Inc(°)	k	a95(°)	N	lat(°)	long(°)	Edad(Ka)	ErrorEdad	Vgplon(°)	VgpLat(°)	Ref:
TAN_04	-	-	-	-	-	19.15	102.32	51	82	-	-	T.S.
TAN_08	350.15	24.79	117.35	5.28	6.00	19.40	102.22	70.00	0.00	159.61	78.59	T.S.
Tan10	1.20	32.80	69.00	7.30	7.00	19.16	102.20	82.00	24.00	60.80	88.27	Maciel <i>et al.</i> , 2010
TAN_02	7.51	46.00	109.17	5.06	7.00	19.16	102.48	110.00	33.00	321.09	79.28	T.S.
Tan11	349.30	43.60	198.00	4.30	7.00	19.01	102.07	163.00	37.00	227.09	78.19	Maciel <i>et al.</i> , 2010
Tan1	7.80	23.80	56.00	16.50	3.00	19.42	102.30	209.00	41.00	54.12	79.76	Maciel <i>et al.</i> , 2010
Tan2	353.50	43.50	199.00	3.90	8.00	19.42	102.30	209.00	41.00	238.28	81.54	Maciel <i>et al.</i> , 2010
Tan6	17.90	58.60	41.00	9.60	7.00	19.43	102.44	256.00	18.00	316.43	64.83	Maciel <i>et al.</i> , 2010
Tan5	348.50	41.20	-	-	2.00	19.39	102.41	269.00	22.00	-	-	Maciel <i>et al.</i> , 2010
Tan4	-	-	-	-	-	19.37	102.37	339.00	23.00	-	-	Maciel <i>et al.</i> , 2010
TAN_01	354.14	31.18	92.10	5.16	8.00	19.03	102.58	347.00	50.00	172.01	84.01	T.S.
Tan7	348.60	28.10	115.00	6.30	6.00	19.31	102.54	373.00	61.00	172.47	78.27	Maciel <i>et al.</i> , 2010
TAN_07	12.68	34.08	46.98	8.34	6.00	19.28	102.38	374.00	31.00	13.12	78.00	T.S.
Tan3	339.90	60.90	242.00	3.60	8.00	19.37	102.08	429.00	64.00	249.41	61.73	Maciel <i>et al.</i> , 2010
Tan8	2.50	27.70	359.00	2.90	8.00	19.26	102.56	612.00	41.00	74.47	84.86	Maciel <i>et al.</i> , 2010
Tan9	352.70	31.30	39.00	9.20	8.00	19.27	102.57	612.00	41.00	174.94	82.67	Maciel <i>et al.</i> , 2010
TAN_06	343.63	19.55	78.19	6.46	6.00	19.27	102.37	768.00	14.00	164.50	71.70	T.S.
TAN_03	10.40	51.21	17.35	7.94	6.00	19.13	102.40	925.00	135.00	311.04	76.30	T.S.
TAN_05	36.20	75.40	189.54	4.40	7.00	19.37	102.49	957.00	157.00	303.43	40.20	T.S.

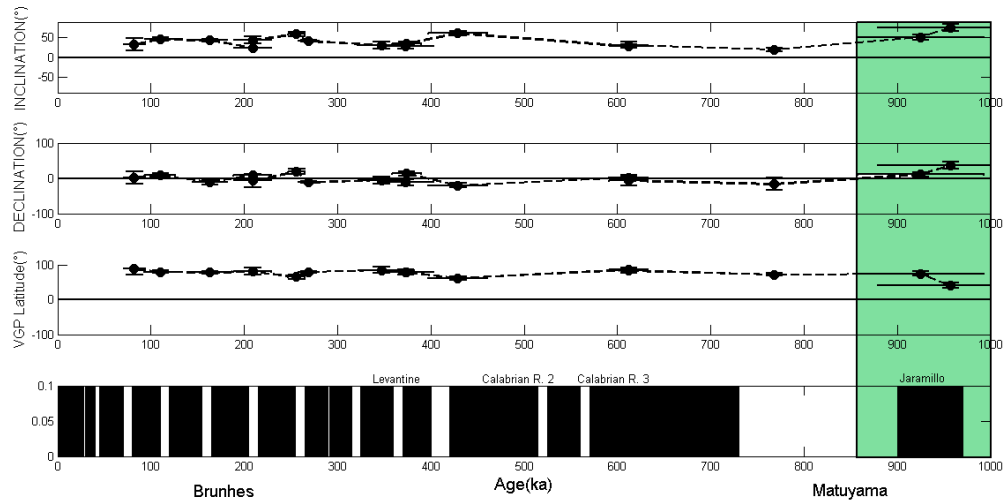


Figure 4. The corresponding VGP of the paleodirection with the mean VGP, and compared with the poles of reference for the last 5 Myr.

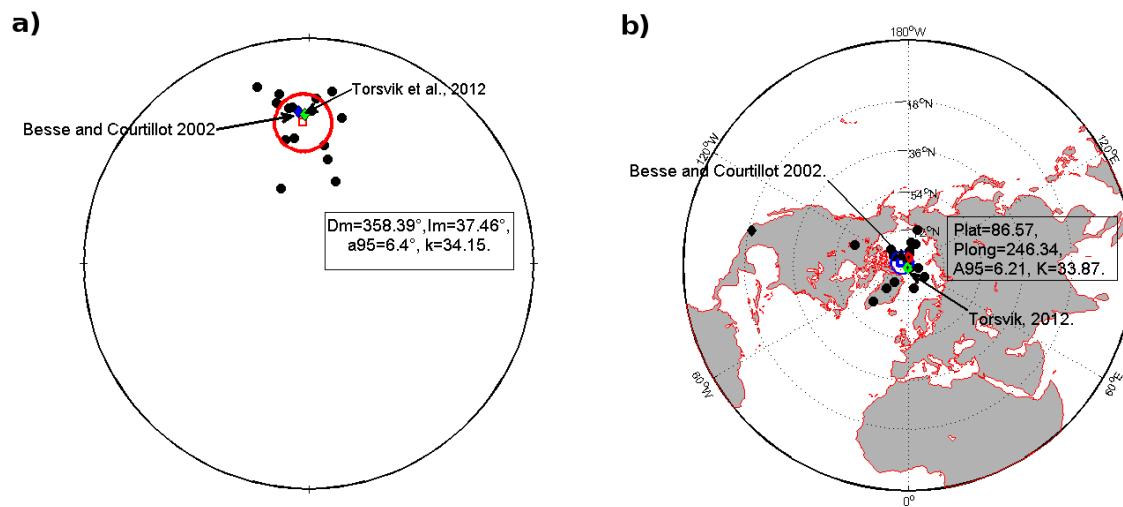


Figure 5. a) Projection of the paleodirection for the Tancitaro volcano with the respective mean paleodirection compared with the direction of reference for the Craton of North America provided by Besse and Courtillot (2002) and Torsvik *et al.*, 2012. b) The corresponding VGP of the paleodirection with the mean VGP, and compared with the poles of reference for the last 5 Myr.

The mean paleomagnetic direction obtained in this study is $I = 37.46^\circ$, $D = 358.39^\circ$, $\alpha_{95m} = 6.4^\circ$, $\kappa = 34.15$, $N = 15$ and (Figure 5a). The corresponding paleomagnetic pole position is $P = 86.57^\circ$, $P_{longm} = 246.34^\circ$, $A_{95m} = 6.21^\circ$ and $K_m = 33.87$ (Figure 5b).

The mean paleodirection obtained was compared with the expected direction derived from the reference pole positions for North American Craton proposed by Besse and Courtillot (2002) and Torsvik *et al.*, (2012) yielding $D_B = 356.1$, $I_B = 33.1$ and $D_T = 358.5$, $I_T = 34.2$ respectively. The use of North

American reference poles is a common practise in almost all previous paleomagnetic surveys (García-Ruiz, *et al.*, 2016, 2017; Maciel *et al.*, 2009, 2014; Ruiz-Martínez *et al.*, 2010.) in order to avoid a kind of bias due to the neotectonic activity. For instance, the San Juanico Buenavista Fault located just beneath Tancitaro Volcano may potentially produce some minor tectonic rotations.

The mean direction agree with the expected directions within the uncertainty and this may be corroborated with the angle of deviation $\delta_B = 4.54$ (with respect to Besse and Courtillot

(2002) reference pole) and $\delta_T=3.34$ (with respect of Torsvik *et al.* (2012) poles). For each paleomagnetic study, it may result useful to calculate the Flattening and Rotation (Butler, 1991) parameters together with their corresponding statistics. These analysis indicate the absence of any important tectonic movement since the values are relatively low $R_B=1.66\pm 7.22$, $F_B=-4.44\pm 6.33$ (for Besse and Courtillot, 2002) and $R_T=-0.73\pm 7.22$, $F_T=-3.34\pm 6.33$ (for Torsvik, 2012). These values also agree to the study carried out by Ruiz-Martínez *et al.* (2010) at different areas within the TMVB, specially for the western and central sectors, where similar small values are obtained ($|R|<6^\circ$ and $|F|<5^\circ$).

Most paleomagnetic studies make the implicit assumption that when averaged over some time interval, the paleomagnetic directions are close to the geocentric axial dipole (GAD) for at least the last 5 Myr, as globally averaged paleopoles should reflect mainly the GAD field (Tauxe and Kent, 2004, Carlot and Courtillot, 1998). Under this assumption, we developed an analysis of TAF and a statistical comparison with the GAD. The mean direction of GAD was calculated for a mean latitude $\lambda=19^\circ 16.08'$ obtaining $D_{GAD}=0^\circ$, $I_{GAD}=34.96^\circ$, yielding a difference of $\Delta I=2.48^\circ$ and $\Delta D=2.32^\circ$. These values are even lower than those found by Maciel *et al.* (2009) in previous studies and reasonably close to the GAD directions. The inclination anomaly found in this study is also compared with the value reported by Lawrence and Constable (2006), for similar latitudes $\lambda=\pm 20^\circ$ as Hawaii, Mexico, South Pacific and Reunion. All these regions yielded statistically indistinguishable values (Figure 6).

PSV analyses are very important to estimate the paleofield location for any time known and when a multiple site sampling is collected the influence of the error is reduced. The PSV analysis was developed complementing the directions presented in this study with the directions of Maciel *et al.* (2014) and the use of angular standard deviation $S_w = \frac{81^\circ}{\sqrt{k}}$, to obtain $S_w=14.09$, the standard deviation as $S_p^2 = (1/N-1)\sum_i \delta_i^2$ which result $S_p=14.33$, the root mean square of the angular deviation of VGP about the geographic axis $S_B = \sqrt{(1/N-1)\sum_i (\delta_i^2 - S_w^2/N)}$ result $S_B=14.33$ with respective lower confidence limit of 13.6 and upper confidence limit 15.61, with the use of the Cox (1970) method.

These results were compared with the model G proposed by McElhinny and McFadden (1997) generated by global paleomagnetic data set of lava flows exclusively. This database was reanalyzed by Johnson *et al.* (2008) using the bootstrap method under the main assumption that the paleomagnetic field closely approximates with the GAD for the last 5 Myr (see also a simplified statistical model Tk03.GAD by Tauxe and Kent (2004)). Our results show a good agreement with the model G proposed by McElhinny and McFadden (1997) (Figure 7) for a latitude of $\lambda=20^\circ$ and a dispersion of $S_M=14$ and it is close to the uncertainty limits of the dispersion for the of Johnson *et al.* (2008) model G, with a value of $S_f=14.8$, but when compared with the Tk03.GAD model some disagreement is observed since this model predicts a low value of $S_f=12.9$ with respect to the $\lambda=20^\circ$ latitude.

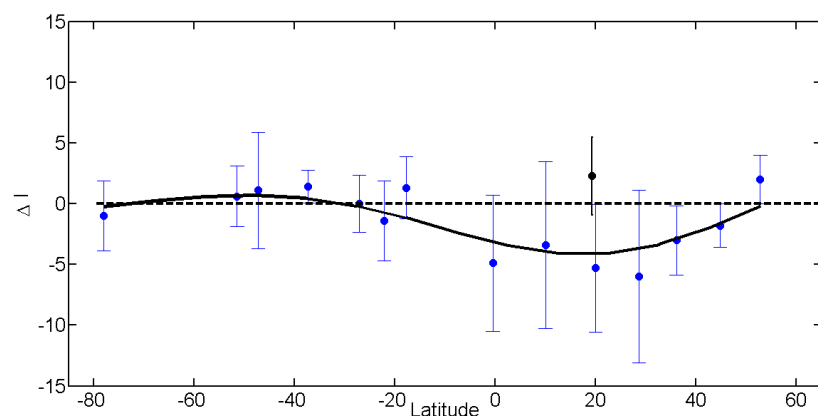


Figure 6. Curve of the best fit with respect of the anomalies of the inclination for several latitudes, with the average of the inclinations anomalies (blue dots) and the anomaly inclination of Tancitaro (Black dot).

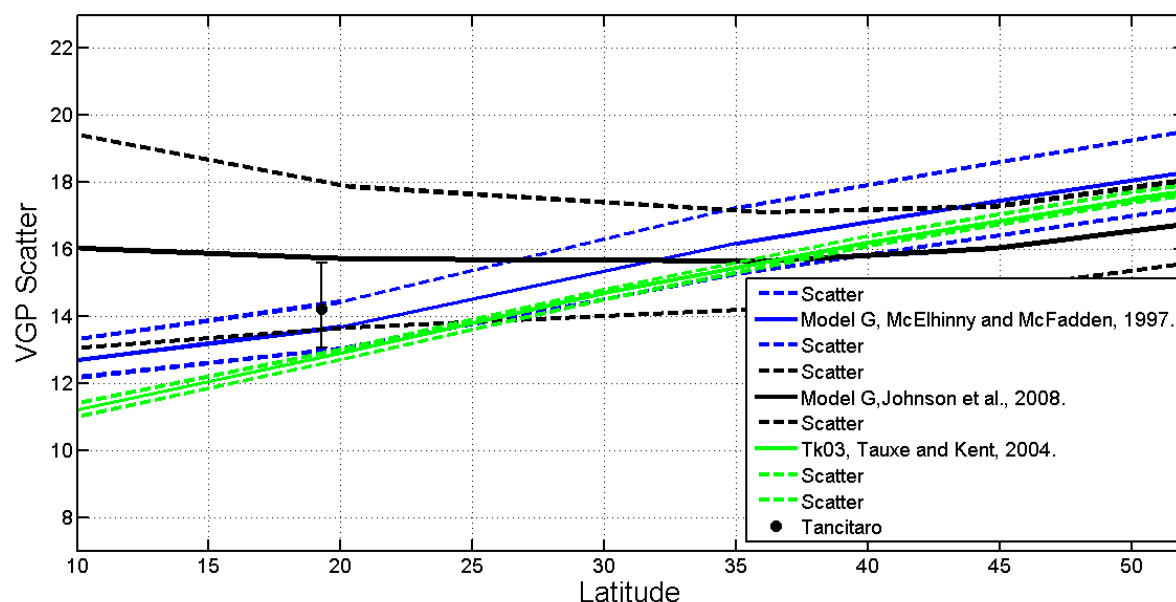


Figure 7. Scatter of the VGP as a function of the latitude for the last 5 Myr, compared with the curves of reference provided by the Model G proposed by McElhinny and McFadden (1997) and Johnson et al. (2008), also with the Tk03.GAD model of Tauxe and Kent (2004).

For the studies developed around of the TMVB, a dispersion $S=15.06\pm0.6^\circ$ and $S=14.9^{14.8}$ was obtained for studies made by Lawrence and Constable (2006) respectively, with dispersion a little bit higher, due the biased to Brunhes Chron.

Two paleodirections obtained on sites Tan-3 and Tan-5 yielded normal polarity paleodirections within reverse polarity Matuyama Chron. They may be erupted during the worldwide observable Jaramillo event (Doell and Dalrymple, 1966; Mankinen and Dalrymple, 1979; Laj and Channel, 2007).

Aeromagnetic data of Tancitaro volcano area was obtained by the Mexican Geological Survey (SGM) in 1999, using the following equipment: Islander Airplane BN2-A21; Geometrics magnetometer G-822A optically pumped cesium vapor with sensitivity of 0.001 nT; data acquisition system, Picodas P-101 AG; Base station magnetometer, GEM Systems GSM-19 Overhauser, sensitivity 0.01 nT; Radar altimeter, Sperry RT-220 Navigation system, GPS Ashtech CG24GPS + Glonass, 16m. Flight parameters were: contour flights at a height of 300 m; direction of flight lines North-South; distance between flight lines 1,000 m; distance between control lines (East-West) 10,000 m; electronic navigation (GPS). The data was initially processed by a digital compilation for

correcting the movement plane (magnetic compensation), and daytime drift. From total magnetic field data the International Geomagnetic Reference Field (IGRF, 1995) was subtracted obtaining the Residual Magnetic Field (RMF, Figure 8)

TMF - IGRF (1995) = RMF. The data were leveled using the control lines and microlevelling. All the processes described above were carried out by the SGM.

From the digital aeromagnetic information of the SGM, we plotted the RMF using the Inclination and Declination data means, in order to calculate the Reduced to the Magnetic Pole (RMP, Figure 9) (Baranov and Naudy, 1964). Based on the RMP, the map of the Derivative in the Z direction was calculated (1 order, Figure 10) (Henderson and Ziets, 1949) and the Upward continuations (Henderson, 1970,) among others.

The location of magnetism sources associated with magmatic chambers is based on the analysis of the contour aeromagnetic map (López-Loera, 2002). This analysis consists the identification of normal bipolar magnetic anomaly near or under the volcanic structure. Once the anomaly is identified, the Baranov and Naudy (1964) algorithm (reduced to magnetic pole) is used in order to locate

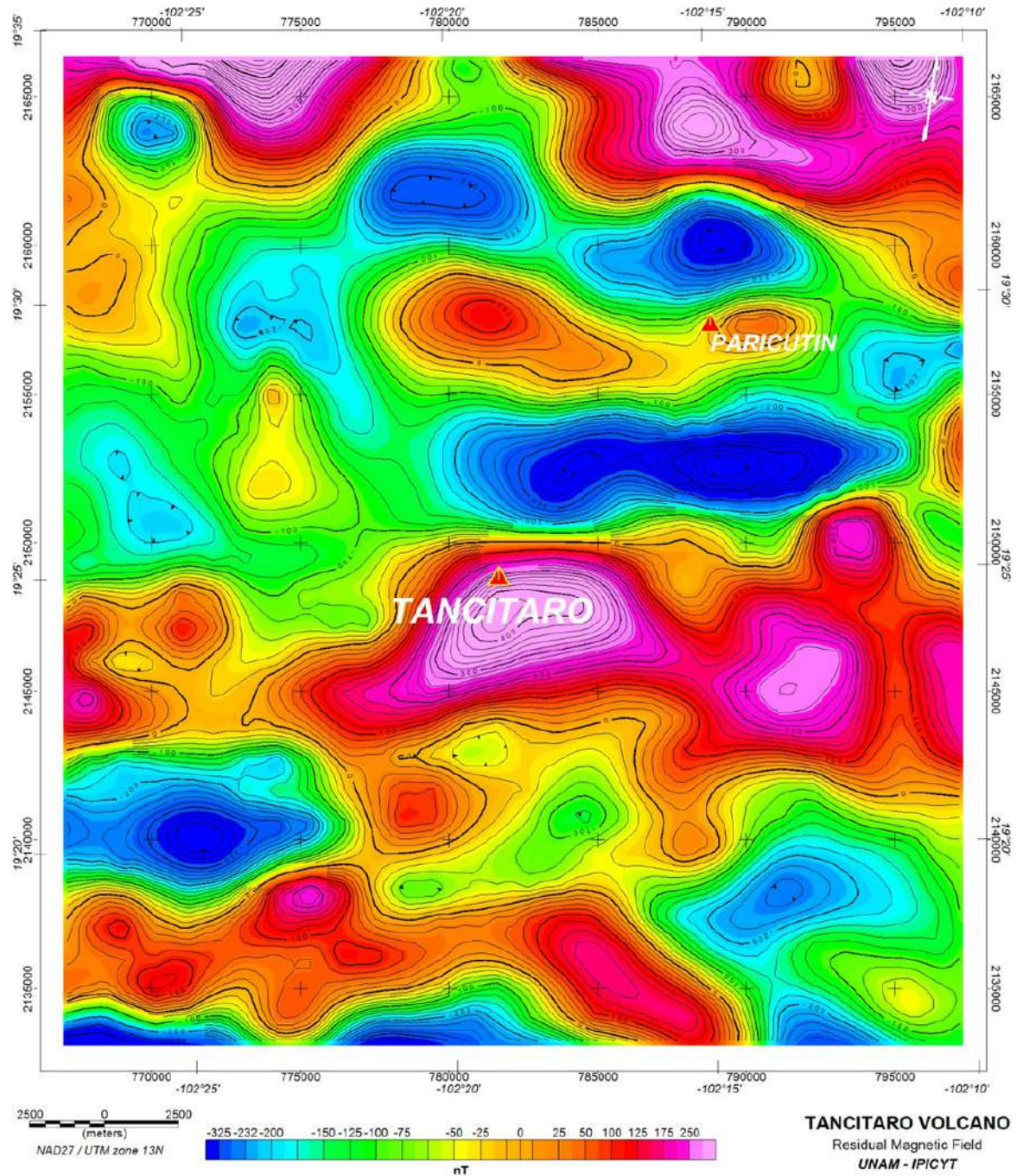


Figure 8. Map showing the calculated Residual Magnetic Field (RMF) of the Tancitaro volcano (TV). The RMF map represents the magnetic field strength with isovalue curves in nT and color range, indicating with red the magnetic highs and with blue the magnetic lows. Note the position of the of the TV with respect to the magnetic anomaly.

precisely the anomaly within the studied body. The so called *Fast Fourier Transform* spectral analysis was used to estimate the depth of the source. This methodology of identification and association of aeromagnetic anomalies with magmatic chambers is based on the fact that the process of cooling of volcanic bodies start from the outside. In this way a crust is formed around the magmatic chamber that allows its identification.

The information processed was configured obtaining the Residual Magnetic Field (RMF, Figure 8). The mean values for the Magnitude in the aeromagnetic survey data (06/1999) was 41,725 nT, the Inclination $46^{\circ}31'$ and declination $7^{\circ}45'$, which means that the RMF anomaly was displaced from the source associated with them. It is a common practice in the processing of aeromagnetic data to use a mathematical algorithm (Baranov and Naudy, 1964) whose application allows to locate the area with respect to the north pole, where the Inclination is 90° and the Declination is 0° and therefore the magnetism sources will be located below the magnetic anomaly.

Contour map of the RMP shows the existence of zones with different magnetization intensities (different colors in Figure 9). This enables to group them into what is called aeromagnetic domains (AMD), López-Loera, 200 TESIS QUITAR2) that can be associated with rocks having similar magnetic susceptibility values. This means that each AMD is associated with a different geological unit. At a regional scale, the entire study area correlates with one AMD, mainly associated with volcanic rocks. At more local scale three aeromagnetic subdomains (AMSD) can be differentiated as described below.

AMSD I. It is located in almost all the study area, it covers the entire central portion and most of the northern side, it is undefined to the E, W and N. It is characterized by the existence of the Tancitaro and Parícutin volcanoes (Figure 9a). It has two large aeromagnetic anomalies (8.8 km x 5 km) elongated in the E-W direction. The anomalies show intensity values of magnetization from 563 to -271.9 nT. One of these anomalies is correlated with the Tancitaro volcano, whose crater is located 1.4 km SW of the center of the aeromagnetic anomaly. In the contour map of the Residual Magnetic Field, this geological structure shows

a normal aeromagnetic anomaly with a 5,450 m of polar distance. According to an analysis of Radial Average Spectrum (Figure 10) the host rock of the magma chamber associated with the Tancitaro volcano is located at depths nearly 2 km., and with the method of average width of the anomaly (Figure 11) it is estimated that the host rock of the magmatic chamber is between 2.6 and 3 km. The Tancitaro volcano shows alignments in all direction, which are associated with weakness zones correlated with faults and/or fractures. Topographically this AMSD I, shows altitudes between 2,031 and 3,792 m, with an average of 2,832 m. Its geological association is with rocks of high magnetic susceptibility such as basalts.

AMSD II. It is located across the southern part of the study area and is mainly characterized by a series of aeromagnetic anomalies associated with magnetic minima, showing values of magnetization intensity from -96 to -650 nT. It has an "E" lying form and is undefined to the S, E and W. Topographically it shows altitudes from 1,140 to 2,141m, with an average of 1,785 m. It correlates with rocks having a low magnetic susceptibility, such as volcanic breccia and pyroclasts.

AMSD III. This subdomain is located towards the NW portion of the studied area, and is undefined to N (Figure 12). It has a form tending to a half circle that shows, in its central portion, an anomaly associated with a magnetic high surrounded by magnetic lows. The values of magnetization intensity are between 197 and -257 nT. Topographically it has altitudes of 1,475 to 2,135 m with an average of 1.780 m. Geologically it correlates with rocks with mean magnetic susceptibilities such as andesitic rocks.

In summary, the aerial magnetometry on the map of Reduce to Magnetic Pole (RMP) shows the existence of three aeromagnetic subdomains all associated with volcanic rocks. The aeromagnetic anomaly associated with the Tancitaro volcano on the map of RMP is shifted 1.4 km to 50° NE and has an area of 5 km (N-S) x 8.8 km (E-W) and a magnetization intensity of 710 nT. The depth of the magmatic chamber correlated with the Tancitaro volcano is interpreted between 3.2 km and 5 km and its shape is elongated in the E-W direction. It is limited in all directions by alignments correlated with faults and/or fractures.

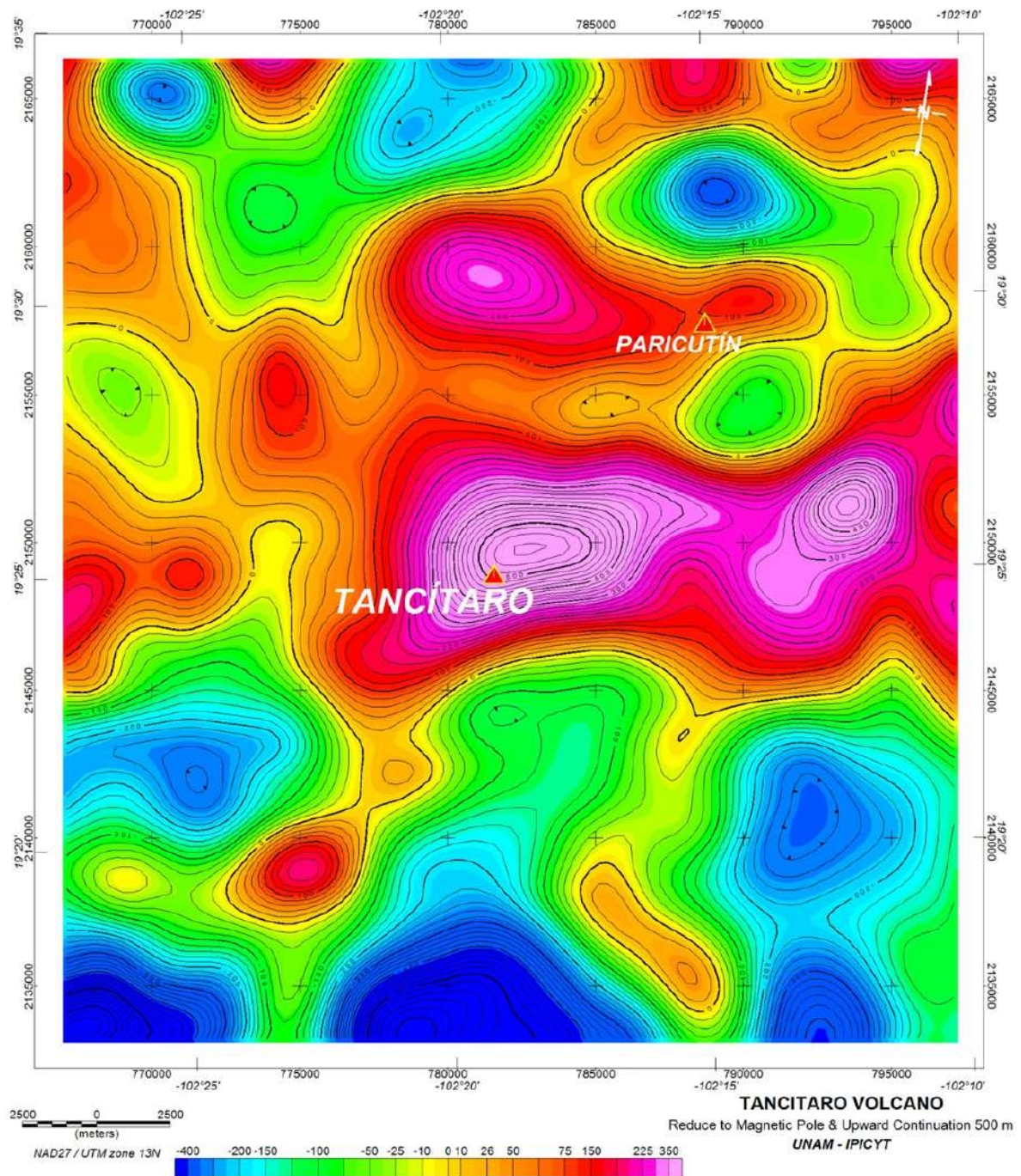


Figure 9. Map of the Reduced to Magnetic Pole (RMP) and Upward Continuation 500 m. The RMP map represents how the study area would be observed if it was located in the north pole, where Inclination is $=90^\circ$ and Declination $=0^\circ$. Note the position of the TV with respect to the magnetic anomaly. In this RMP the anomalies move to the north.

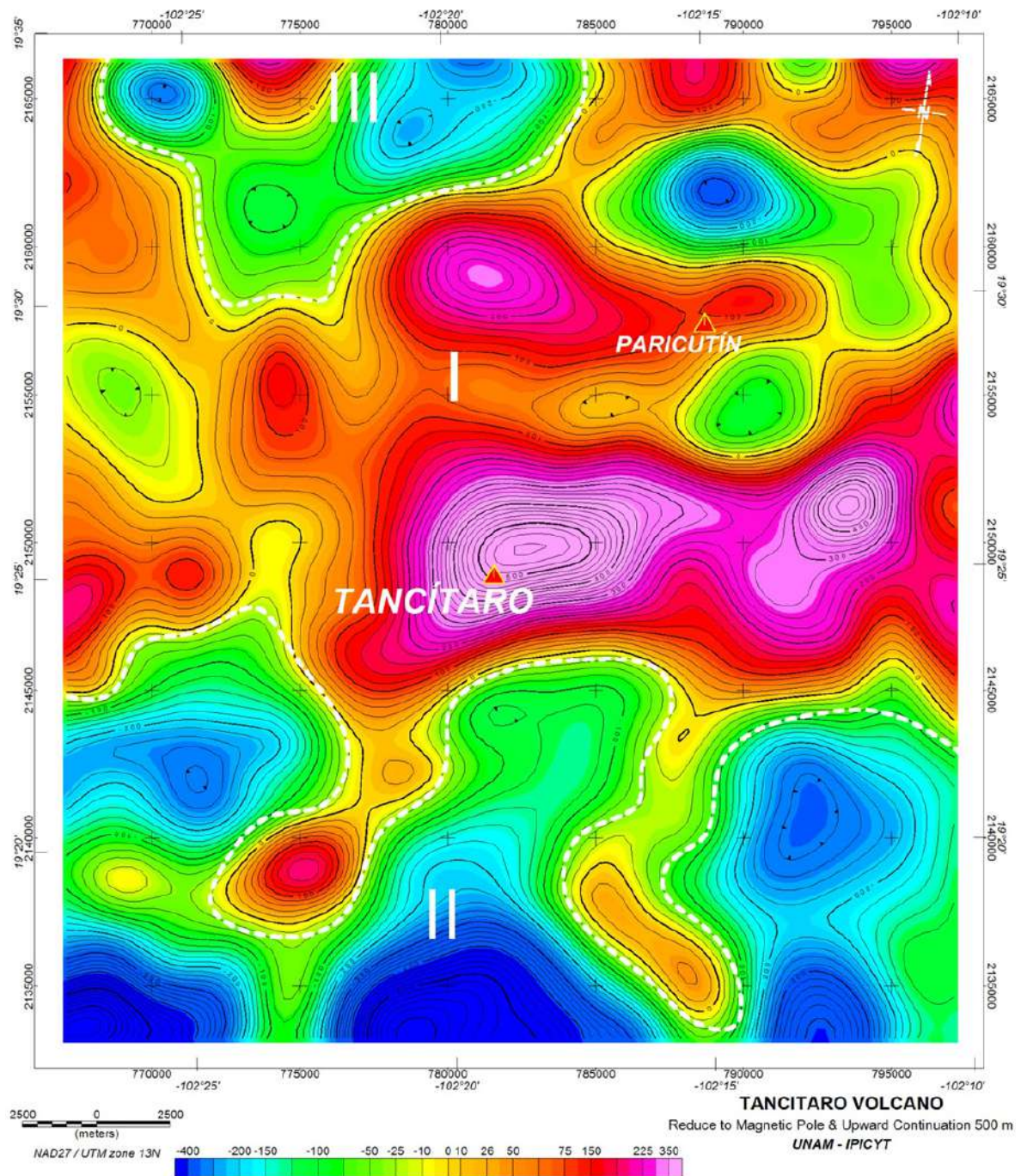


Figure 9a. Map of the Reduced to Magnetic Pole (RMP) and Upward Continuation 500 m and aeromagnetic subdomains AMSD (I, II and III) of the Tancitaro volcano (TV) and surrounding areas. The AMSD represents a zone with similar magnetic susceptibility.

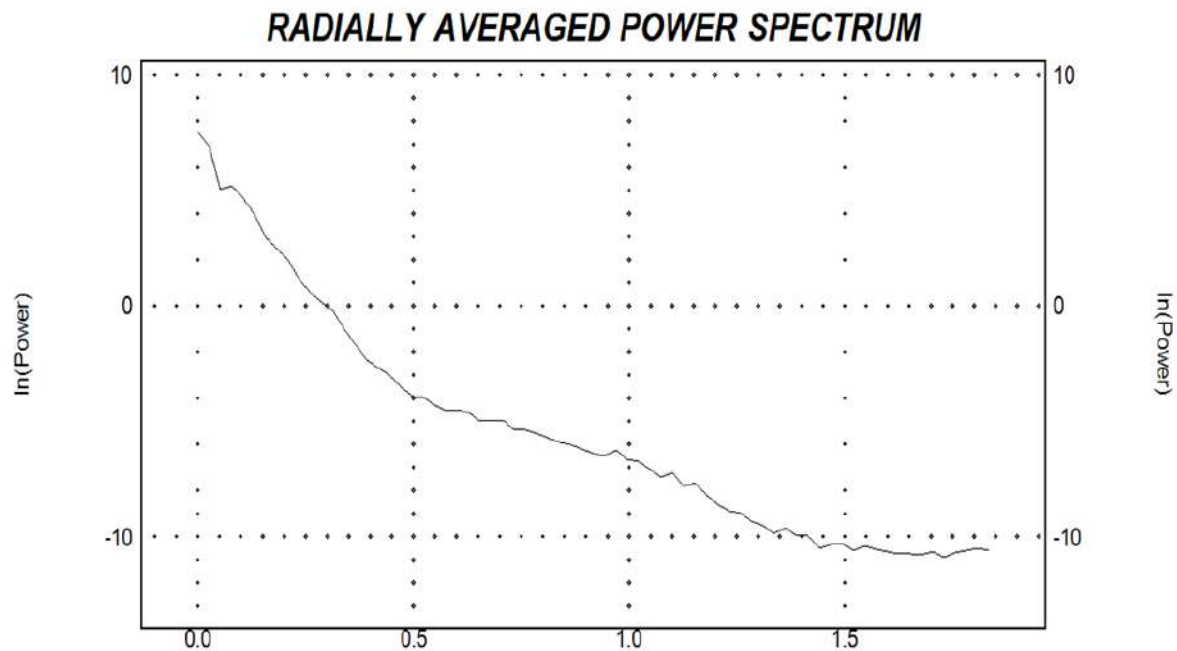


Figure 10. The profile represents the Radially Averaged Power Spectrum of the study area.

Conclusions

A detailed rock-magnetic and paleomagnetic study was carried out on the lava flows associated to the Tancitaro volcano in order to contribute both to the new generation Time Averaged Paleomagnetic Field database and to estimate the latitudinal dependence of the paleosecular variation through the virtual geomagnetic pole scatter. The combined dataset incorporating previously reported paleodirections from the same area offer a detailed record of the Earth's Magnetic Field fluctuation for the last 1 My.

Mean paleodirections was found reasonably close to the Geomagnetic Axial Dipole directions and statistically indistinguishable from the expected directions derived from the stable North America which attest that there is no major tectonic deformations occurred during the last 1 My according to the previous studies. All samples yielded well defined normal polarity magnetization. Two flows are correlated to the Jaramillo polarity event, which provide a useful marker for the volcanic activity in the MGVE.

Combined aeromagnetic survey shows the existence of three magnetic subdomains all associated with volcanic rocks. The aeromagnetic anomaly associated with the Tancitaro volcano on the map of RMP is shifted 1.4km to the Northeast 50° and has an area of 5km (North-South) 8.8km (East-West) and shows a magnetization intensity of 710 nT. The depth of the magmatic chamber correlated with the Tancitaro volcano is interpreted between 3.2km and 5km and the shape is elongated in the East-West direction. It is limited in all directions by alignments correlated with faults and/or fractures, but this could be inside the flows or formed after the events of interest in the geological maps of the Geological National Service, in the paleomagnetic results this relationship was not observed that could be reflected not being near the direction of reference or the GAD.

Acknowledgments

The financial support was given by UNAM-PAPIIT project IN10524 and CONACyT Ciencia Basica (00131191).

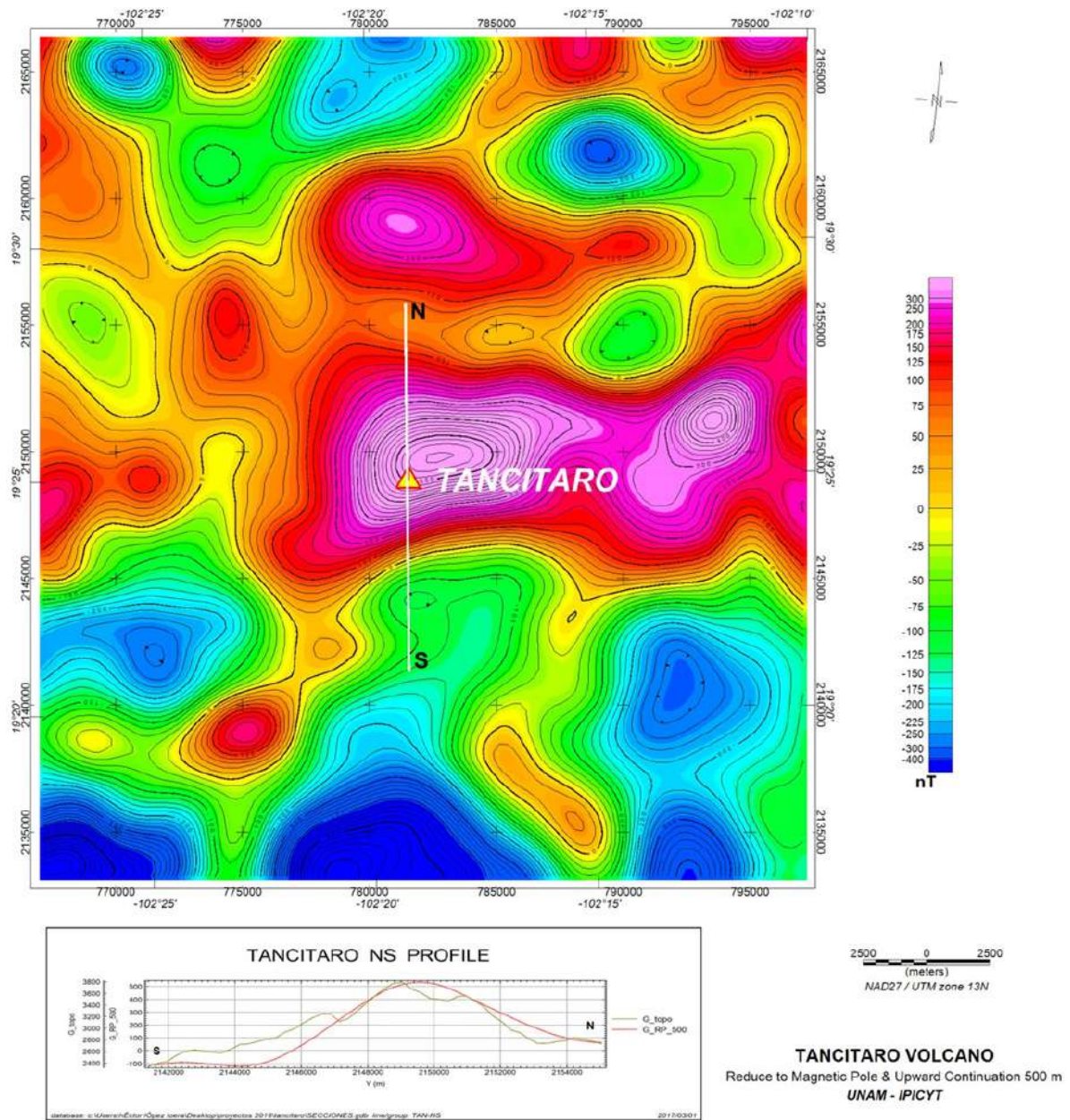


Figure 11. The profile observed with NS direction in the map of the RMP & Upward Continuation 500 m; the same as shown in the lower side of the map and that served as base to estimate the depth of the source of the magnetic anomaly with the average width method.

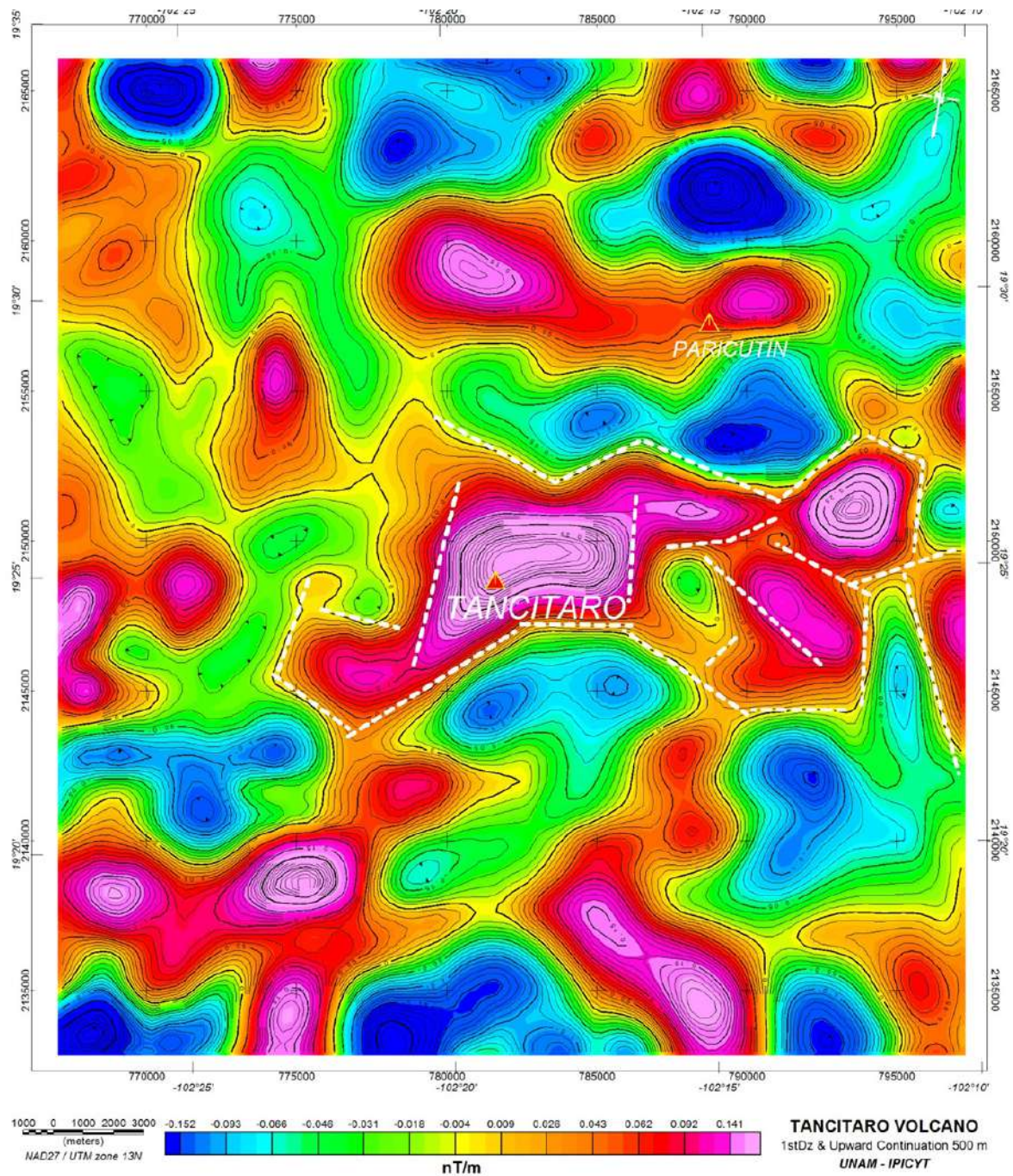


Figure 12. First derivative in Z direction and upward continuation 500 m map. This map shows the alignments (white color lines) associated with the anomaly of Tancitaro volcano. These alignments are correlated with faults and/or fractures.

References

- Aiken, C., and Z. Peng (2014). Dynamic triggering of microearthquakes in three geothermal/volcanic regions of California. *J. Geophys. Res. Solid Earth*, 119, 6992-7009.
- Baranov, V., and Naudy, H., 1964. Numerical calculation of the formula of reduction to the magnetic pole. *Geophysics*, v. 29, p. 67-79.
- Besse, J., Courtillot, V., 2002, Apparent and true polar wander and the geometry of the magnetic field in the last 200 million years, *Journal of Geophysical Research*, v. 107, no. B11, 2300.
- Butler R.F, 1991, *Paleomagnetism: Magnetic Domain to Geologic Terranes.*, Book, Blackwell Science.
- Carlut, J., and V. Courtillot, 1998, How complex is the time-averaged geomagnetic field over the past 5 Myr?, *Geophys. J. Int.*, v. 134, p. 527-544.
- Connor, C.B., 1987. Structure of the Michoacán-Guanajuato volcanic field, Mexico. *J. Volcanol. Geotherm. Res.* v. 33, p. 191-200.
- Chandra, S., H. Khurshid, M. H. Phan, and H. Srikanth (2012), Asymmetric hysteresis loops and its dependence on magnetic anisotropy in exchange biased Co/CoO core-shell nanoparticles, *Appl. Phys. Lett.*, 101(23), 8-13, doi:10.1063/1.4769350.
- Connor, C.B., 1990. Cinder cone clustering in the TransMexican Volcanic Belt: implications for structural and petrologic models. *J. Geophys. Res. Solid Earth* (1978-2012), v. 95 no. (B12), p. 19395-19405.
- Cox, A., 1970, Confidence limits for the precision parameter k. *Geophysical Journal of the Royal Astronomical Society*, v. 18, p. 545-549.
- Doell, RR and Dalrymple, GB (1966). Geomagnetic polarity epochs: A new polarity event and the age of the Brunhes-Matuyama boundary. *Science*, v. 152, p. 1060-1061.
- Dunlop David J., 2002, Theory and application of the Day plot (Mrs/Ms versus Hcr/Hc) 2. Application to data for rocks, sediments, and soils. *Journal of Geophysical Research*, v. 107, no. B3, p. 2057, doi:10.1029/2001JB000487.
- Fisher R.A., 1953, Dispersion on a sphere. *Proceedings of the Royal Society of London A*, v.217, p. 295-305.
- García-Ruiz R., Goguitchaichvili A., Cervantes-Solano M., Cortés-Cortés A., Morales-Contreras J., Maciel-Peña R., Rosas-Elguera J. and Macías-Vázquez J. L., 2016, Secular variation and excursions of the Earth magnetic field during the Plio-Quaternary: New paleomagnetic data from radiometrically dated lava flows of the Colima volcanic complex (western Mexico), *Revista Mexicana de Ciencias Geológicas*, v. 33, no. 1, p., 72-80.
- García-Ruiz R., Goguitchaichvili A., Cervantes-Solano M., Morales J., Maciel-Peña R., Rosas-Elguera J., Cejudo-Ruiz R., and Urrutia-Fucugauchi J., AÑO??? Rock-Magnetic and paleomagnetic survey on dated lava flows erupted during the Brunhes and Matuyama chrons: the Mascota Volcanic Field revisited (Western Mexico), *Stud. Geophys. Geod.*, v. 61, doi: 10.1007/s11200-016-0148-6 (in press).
- Hasenaka, T., Carmichael, I.S., 1985. The cinder cones of Michoacán-Guanajuato, central Mexico: their age, volume and distribution, and magma discharge rate. *J. Volcanol. Geotherm. Res.* v. 25, p. 105-124.
- Hasenaka, T., Ban M. and Delgado-Granados H., 1994, Contrasting volcanism in the Michoacán-Guanajuato Volcanic Field, central Mexico: Shield volcanoes vs. cinder cones. *Geophysical International*, v.33, no.1, pp.125- 138.
- Hasenaka, T., 1994. Size, distribution, and magma output rate for shield volcanoes of the Michoacán-Guanajuato volcanic field, Central Mexico. *Journal of Volcanology and Geothermal Research*, v. 63, p.13-31.
- Henderson, R. G., 1970. On the Validity of the use of Upward Continuation Integral for Total Magnetic Intensity Data. *Geophysics*, V. 35, 5, 916-919.
- Henderson, R. G. and Zietz, I., 1949. The computation of second vertical derivatives of geomagnetic fields, *Geophysics*, v. 14, p. 508-516.

- IGRF, 1995, International Geomagnetic Reference Field. *IAGA Division V-Mod, Geomagnetic Field Modeling*.
- Johnson, CL., Constable G., Tauxe L. *et al.*, 2008, Recent investigations of the 0-5 Ma geomagnetic field recorded in lava flows. *Journal of the Earth Sciences, Geochem. Geophys. Geosyst.*, v. 9, no. 4, p. 1525-2027, Q04032.
- Kirschvink, J.L., 1980, The least-square line and plane and analysis of paleomagnetic data. *Geophysical Journal International*, v. 62, no. 3, p. 699-718.
- Laj C. and Channell J.E.T., 2007, Geomagnetic excursions, *Treatise on Geophysics, Geomagnetism*, Elsevier, v. 5, p. 373 - 416.
- Lawrence K. P. and Constable C. G., 2006. Paleosecular variation and the average geomagnetic field at latitude., *Geochemistry Geophysics Geosystems*, *Journal of the Earth Sciences*, v. 7, no. 7.
- Leonhardt R., 2006, Analyzing rock magnetic measurements: The RockMagAnalyser 1.0 software, *Computer and Geosciences*, v. 32, p. 1420-1431.
- López-Loera, H., 2002. Estudio de las Anomalías Magnéticas y su relación con las Estructuras Geológicas y Actividad Eruptiva de los Complejos Volcánicos Activos de Colima e Izta-Popocatepetl, México. Tesis Doctoral, Instituto de Geofísica, UNAM. Pp 235.
- Maciel, P. R., Goguitchaichvili, A., Garduño Monroy V. H., Ruiz Martínez V. C., Reyes Aguilar B., Morales J., Alva-Valdivia L., Miranda Caballero C., and Urrutia-Fucugauchi J., 2010, Paleomagnetic and rock-magnetic survey of Brunhes lava flows from Tancitaro volcano, México, *Geophysical International*, v. 48, no. 4, pp. 375-384.
- Maciel P. R., Goguitchaichvili A., Marie-Noëlle G., Ruiz-Martínez V. C., Calvo R. M., Siebe C., Aguilar R., B., and Morales J., 2014, Paleomagnetic secular variation study of Ar-Ar dated lavas flows from Tacambaro área (Central Mexico): Possible evidence of Intra-Jaramillo geomagnetic excursion in volcanic rocks, *Physics of the Earth and Planetary Interiors*, v. 299, p. 98-109.
- Mankinen EA and Dalrymple GB (1979). Revised Geomagnetic polarity time scale for the interval 0-5 m.y.b.p. *Journal of Geophysical Research* v. 84, p. 615-626.
- McElhinny, M.W., McFadden, P.L., 1997, Paleosecular variation over the past 5 Myr based on a new generalized database. *Geophysical Journal International*, 203(2), 240-252.
- Moskowitz B. M., 1981, Methods for estimating Curie temperatures of titanomagnetites from experimental Js-T data., *Earth and Planetary Sciences Letters.*, v. 53, no. 1, p. 84-88.
- Ownby, S. E., H. Delgado-Granados, R. A. Lange and C. M. Hall, 2007. Volcan Tancitaro, Michoacan, Mexico, 40ar/39ar constraints on its history of sector collapse. *J. Volcanology and Geothermal Res.*, v. 161, no. 1-2, p. 1-14.
- Ownby S. E., Lange R. A., Hall C. M., and Delgado-Granados H., 2010, Origin of andesite in the deep crust and eruption rates in the Tancitaro-Nueva Italia Region of the central Mexican arc., *Geological Society of America Bulletin*, v. 123, no. 1-2, p. 274-294.
- Prévot, M., Mankinen E. A., Gromme S. C., Coe R. S., 1985, How the geomagnetic field vector reverses polarity. *Nature*, v. 316, no. 6025, p. 230-234.
- Rodríguez-Ceja M., Goguitchaichvili A., Calvo-Rathert M., Morales-Contreras J., Alva-Valdivia L., Rosas E. J., Urrutia F. J., and Delgado G. H., 2006, Paleomagnetism of the Pleistocene Tequila Volcanic Field (Western Mexico), *Earth Planets Space*, v. 58, p. 1349-1358.
- Ruiz-Martínez V.C., Urrutia-Fucugauchi J., and Osete M. L., 2008 en pag 6 OJO, Palaeomagnetism of the Western and Central sectors of the Trans-Mexican volcanic belt-implications for tectonic rotations and palaeosecular variation in the past 11 Ma, *Geophysical Journal International*, v. 180, p. 577-595, doi:10.1111/j.1365-246X.2009.04447.x.
- Tauxe, L. (1998). *Paleomagnetic Principles and Practice*. Dordrecht: Kluwer Academic Publishers.

Tauxe L., and Kent D.V., 2004, A Simplified Statistical Model for the Geomagnetic Field and Detection of Shallow Bias in Paleomagnetic Inclinations: Was the ancient Magnetic Field Dipolar?: *Wiley Online Library*, pp. 101-113.

Torsvik, T.H., van der Voo, R., Preeden, U., Mac Niocail, C., Steinberger, B Hinsbergen, B., Doubrovine, P. V., van Hinsbergen, D.J.J., Domier, M., Gaina, C., Tohver, E., Meert, J.G., McCausland, P.J.A., Cocks, L.R.M., 2012, Phanerozoic polar wander, palaeogeography and dynamics, *Journal Earth-Science Reviews*, v. 114, pp. 325-368.